Performance improvement of InGaN blue light-emitting diodes with several kinds of electron-blocking layers*

Chen Jun(陈 峻)[a)b)], Fan Guang-Han(范广涵)[a)†], Zhang Yun-Yan(张运炎)[c)], Pang Wei(庞 玮)[b)], Zheng Shu-Wen(郑树文)[a)], and Yao Guang-Rui(姚光锐)[a)]

[a)] *Institute of Opto-Electronic Materials and Technology, South China Normal University, Guangzhou* 510631, *China*

[b)] *Experimental Teaching Center, Guangdong University of Technology, Guangzhou* 510006, *China*

[c)] *Department of Electronic and Computer Engineering, The Hong Kong University of Science and Technology, Hong Kong, China*

(Received 14 August 2011; revised manuscript received 12 November 2011)

The performance of InGaN blue light-emitting diodes (LEDs) with different kinds of electron-blocking layers is investigated numerically. We compare the simulated emission spectra, electron and hole concentrations, energy band diagrams, electrostatic fields, and internal quantum efficiencies of the LEDs. The LED using AlGaN with gradually increasing Al content from 0% to 20% as the electron-blocking layer (EBL) has a strong spectrum intensity, mitigates efficiency droop, and possesses higher output power compared with the LEDs with the other three types of EBLs. These advantages could be because of the lower electron leakage current and more effective hole injection. The optical performance of the specifically designed LED is also improved in the case of large injection current.

Keywords: electron-blocking layer, light-emitting diode, internal quantum efficiency

PACS: 85.60.Jb, 85.50.–n, 87.15.A–, 78.60.Fi **DOI:** 10.1088/1674-1056/21/5/058504

1. Introduction

In recent years, great progress has been made in developing high-efficiency high-power InGaN blue light-emitting diodes (LEDs). Because of the high efficiency of photoelectric conversion, they have wide applications, including in full-color displays, liquid-crystal display back-lighting, and white solid-state lamps.[1−3] However, efficiency droop[4−10] has become a troublesome issue. Various mechanisms have been suggested, including junction heating,[11] Auger recombination,[12,13] carrier delocalization occurring at high excitation intensities,[14,15] low hole injection,[16,17] and electron leakage out of the multi-quantum well (MQW) active region.[5]

On the other hand, the conventional electron-blocking layer (EBL) is usually regarded as being indispensable for the InGaN blue LED[18−26] to suppress the electron leakage current and improve the optical performance of the LED. However, recent research suggests that a serious downward band-bending[6] caused by the strong polarization near the last barrier and the EBL is obvious. As a result, the EBL that acts as a potential barrier for electrons fails to reach its original purpose. It is also reported that this band-bending will lead to a larger potential barrier for holes at the same time, which results in the difficulty in injecting holes.[27] The purpose of this work is to enhance the hole injection efficiency, suppress the electron leakage current, and mitigate efficiency droop. Several specific designs for the EBLs in the InGaN blue LEDs are investigated numerically. The mechanisms of electron and hole transportation, the carrier confinement, and the electrostatic field distribution behind these improvements are discussed.

2. Experiment

The optical and physical properties of the LEDs are investigated numerically with the APSYS (advanced physical models of semiconductor devices)[28] simulation software. The conventional LED (structure

*Project supported by the National Natural Science Foundation of China (Grant No. 61176043), the Fund for Strategic and Emerging Industries of Guangdong Province, China (Grant No. 2010A081002005), and the Project of Combination of Production and Research of the Education Ministry and Guangdong Province, China (Grant No. 2010B090400192).

†Corresponding author. E-mail: gfan@scnu.edu.cn

© 2012 Chinese Physical Society and IOP Publishing Ltd

A) shown in Table 1 is used in this paper as the reference. It is grown on a *c*-plane sapphire substrate by metal-organic chemical vapor deposition (MOCVD). A 50 nm undoped GaN layer and a 4.5 μm n-type GaN layer (n-doping=5×10^{18} cm^{-3}) are subsequently deposited first. The active region consists of four pairs of quantum wells, including four 2.2 nm $In_{0.1}Ga_{0.9}N$ wells and five 15 nm GaN barriers. The barriers are undoped except for the first one close to the n-layer, which is n-doped (n-doping=5×10^{18} cm^{-3}), and the last one close to the p-layer, which is p-doped (p-doping=7×10^{17} cm^{-3}). A 20 nm p-type $Al_{0.2}Ga_{0.8}N$ and a 0.2 μm p-type GaN cap layer (p-doping=7×10^{17} cm^{-3}) are then deposited on the top of the active region. The area of the device is 300 μm×300 μm. In order to mitigate the efficiency droop and improve the performance of the LED, we investigate three specific epitaxial structures, which are similar to the conventional one except for the EBL structure. The second epitaxial structure (structure B) does not have the EBL, as shown in Table 2. In the third structure (structure C), the $Al_{0.2}Ga_{0.8}N$ EBL used in the conventional LED is replaced by an $In_{0.18}Al_{0.82}N$ EBL, as shown in Table 3. And the last structure (structure D) adopts the AlGaN layer with Al content gradually increasing from 0% to 20% as the EBL. The details of structure D are listed in Table 4. In our simulation, the light extraction efficiency is assumed to be 0.78 in order to match the optical performance of the experimental data.[29] The band offset ratio is assumed to be 0.7/0.3.[30] And the material parameters are chosen to be the same as those in Ref. [31]. The other simulation parameters are set to be the same as those in Ref. [32].

Table 1. Schematic of the conventional LED (structure A).

p-GaN, 0.2 μm, 7×10^{17} cm^{-3}
EBL, p-$Al_{0.2}Ga_{0.8}N$, 0.02 μm, 7×10^{17} cm^{-3}
MQW, $In_{0.1}Ga_{0.9}N$/GaN (2.2 nm/15 nm), four-pairs
n-GaN, 4.5 μm, 5×10^{18} cm^{-3}
undoped-GaN, 50 nm, nucleation layer
sapphire substrate

Table 2. Schematic of the LED without EBL (structure B).

p-GaN, 0.2 μm, 7×10^{17} cm^{-3}
MQW, $In_{0.1}Ga_{0.9}N$/GaN (2.2 nm/15 nm), four-pairs
n-GaN, 4.5 μm, 5×10^{18} cm^{-3}
undoped-GaN, 50 nm, nucleation layer
sapphire substrate

Table 3. Schematic of the LED using an $In_{0.18}Al_{0.82}N$ EBL (structure C).

p-GaN, 0.2 μm, 7×10^{17} cm^{-3}
EBL, p-$In_{0.18}Al_{0.82}N$, 0.02 μm, 7×10^{17} cm^{-3}
MQW, $In_{0.1}Ga_{0.9}N$/GaN (2.2 nm/15 nm), four-pairs
n-GaN, 4.5 μm, 5×10^{18} cm^{-3}
undoped-GaN, 50 nm, nucleation layer
sapphire substrate

Table 4. Schematic of the LED using AlGaN with gradually increasing Al content as the EBL (structure D).

p-GaN, 0.2 μm, 7×10^{17} cm^{-3}
EBL, p-$Al_xGa_{1-x}N$ ($x:0\sim0.2$), 0.02 μm, 7×10^{17} cm^{-3}
MQW, $In_{0.1}Ga_{0.9}N$/GaN (2.2 nm/15 nm), four-pairs
n-GaN, 4.5 μm, 5×10^{18} cm^{-3}
undoped-GaN, 50 nm, nucleation layer
sapphire substrate

3. Results and discussion

Figure 1 shows the electrostatic fields of the active region near the last QW barrier and the EBL with an injection current of 150 mA. As can be seen from the figure, structure A (the thick solid line) has the largest electrostatic field among the four LED structures. A strong piezoelectric polarization field is generated in structure A because of the severe lattice mismatch between the last GaN barrier and the AlGaN EBL. Structure C (short dashed line) has a smaller electrostatic field than that of structure A, because the InAlN EBL can achieve a higher quality of lattice-match to GaN. Moreover, the electrostatic field in structure D (short dotted line) is much smaller than that of structures A and C. It shows that the EBL of structure D can significantly lower the degree of polarization by using the AlGaN with gradually increasing Al content. The electrostatic field near the last barrier is almost unobservable in structure B, because it does not have an EBL.

Figure 2 shows energy band diagrams of the LEDs with various EBLs at 150 mA. As shown in Fig. 2(a), the electrostatic polarization field pulls down the energy band at the interface of the last GaN barrier and the AlGaN EBL. As a result, the effective potential barrier height (260 meV) for electrons is reduced, and the electrons cannot be confined in the QWs effectively and will spill over from the p-layer. When the AlGaN EBL is replaced by the InAlN EBL in structure C, the effective potential height (673 meV) for

electrons is increased obviously. In addition, structure D has the highest effective potential height (794 meV) for electrons among the four structures, as shown in Fig. 2(d). Consequently, the effective potential height for the electrons is dependent on the electrostatic field and the downward band-bending in the active region of the LED.

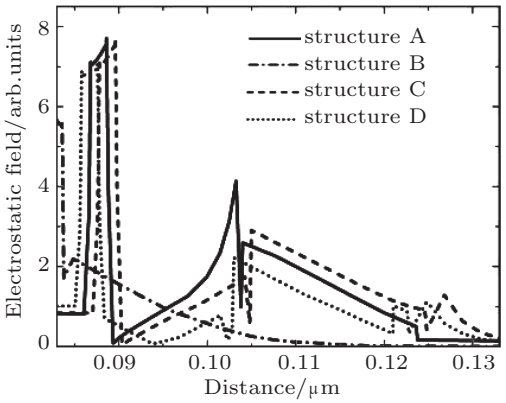


Fig. 1. The electrostatic fields of LEDs near the last QW barrier and the EBL with an injection current of 150 mA, showing a small location shift on the horizontal axis.

In addition, because of the serious band-bending near the last barrier and the EBL caused by the polarization field, the EBL also acts as a potential barrier for holes, which can block the hole injection from the p-layer. As shown in Fig. 2, the effective potential height (644 meV) for holes between the last barrier and the EBL in structure A is much higher than those of the other three LED structures (368 meV for structure B, 531 meV for structure C, and 488 meV for structure D). This implies that it is much harder for the holes to be injected into the active region in the conventional LED (structure A) due to blocking of the effective potential barrier. As for structures C and D, the downward band-bendings are mitigated compared with those of the conventional one, and the effective potential barrier heights for holes are lowered, thereby enhancing hole injection efficiency. It is worth noting that the downward band-bending is almost eliminated and the hole injection is enhanced in structure D. Structure B has the lowest effective potential height for holes and the smallest electrostatic field near the last QW barrier because no EBL is used, but that does not make the optical performance of structure B better than that of the other structures. The reason for this will be discussed later.

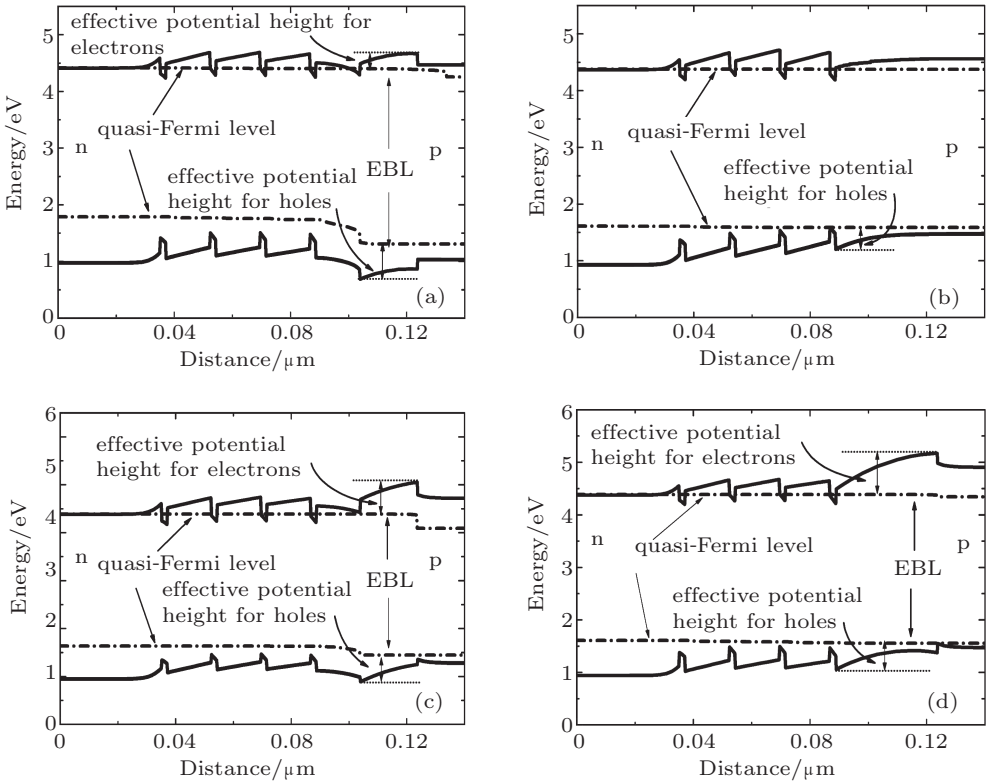


Fig. 2. Energy band LED diagrams for structures (a) A, (b) B, (c) C, and (d) D, with an injection current of 150 mA.

Figure 3 shows the carrier concentration distributions of the LEDs with an injection current of 150 mA. In GaN-based materials, the electron has a small effective mass and a high mobility. This is convenient for the transport of electrons in the active region. As shown in Fig. 3(a), the distributions of electron concentration in the active regions are quite uniform in structures A, C, and D. However, it is also easier for the the electrons to spill out of the p-layer for the same reason. The conventional AlGaN EBL is not effective in suppressing electron leakage current, as shown in Fig. 3(a) by the dashed-dotted line. The electron leakage becomes worse in structure B (thin solid line) when no EBL is adopted, and even the electron concentrations in the four QWs of structure B decrease from the n-layer to the p-layer because the large electrons spill over from the active region. When the InAlN layer is used as the EBL (structure C), the higher effective potential barrier of the EBL makes the electrons more effectively confined, and the electron leakage current decreases obviously, as shown in Fig. 3(a) by the short dotted line. The lowest electron leakage current is achieved in structure D (thick solid line) by using the AlGaN with gradually increasing Al content. This is due to the highest effective potential barrier height for electrons in the conduction band (shown in Fig. 2).

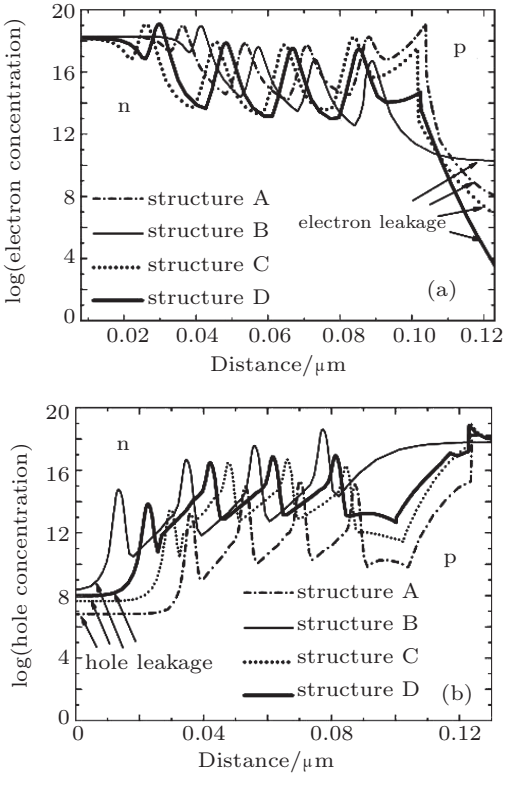


Fig. 3. (a) Electron and (b) hole concentration distributions in structures A, B, C, and D with an injection current of 150 mA.

It is noted that in Fig. 3(b), the hole concentration in structure B (thin solid line) is much higher than that in the three other structures. This shows a high efficiency of hole injection in the structure without EBL, which also means that the EBL indeed acts as an impediment to hole injection. Among structures A, C, and D, structure D has the highest hole concentration, and the hole concentration as well as the hole injection efficiency approaches that of structure B. This is because the effective potential barrier height for the holes in the valence band of EBL is smaller (Fig. 2(d)) and the holes are easier to move into the active region. On the contrary, structure A has the lowest hole concentration and the worst hole injection efficiency because of the serious impediment of the highest effective potential barrier for holes in the valance band caused by the AlGaN EBL. Structure C is better than structure A due to the lower height of the effective potential barrier for holes achieved by replacing the AlGaN EBL with the InAlN one.

Figure 4 shows the EL spectra, the internal quantum efficiencies (IQEs), and the output powers of the four LED structures. The peaks are at the same wavelength, and they are shifted along the horizontal axis in Fig. 4(a) for better comparison. Although the hole concentration in structure B is higher than that in the other structures (Fig. 3(b)), the large electron spilling over from the p-layer means that very few electrons become confined in the QWs and participate in the recombination with holes. As a result, structure B (thin solid line) has the smallest spectrum intensity, the worst efficiency droop (74.7%), and the lowest output power of the four structures shown in the figure. The optical performance of the conventional LED is not improved much when the AlGaN layer acts as the EBL (dashed-dotted line). The efficiency droop is 64.6%, and the output power drops quickly after the current density reaches 230 A/cm^2, and becomes even lower at 300 A/cm^2. This shows that the confinement of the carriers using a conventional AlGaN EBL is not sufficiently effective and that the benefits are very limited compared with the structure without the EBL. When the AlGaN EBL is replaced by the InAlN EBL, which has a better lattice-match quality to the GaN barrier, in structure C (short dotted line) the spectrum intensity is enhanced remarkably, and the efficiency droop decreases to 23.4%, as shown in the figure. The best optical performance among the four structures is obtained in structure D by using the AlGaN with gradually increasing Al content. The ef-

ficiency droop is mitigated remarkably to the lowest value of 12.2%, and the biggest luminous intensity and highest output power are realized in this structure. In addition, the output power is high and maintains the increasing trend with increasing injection current. This indicates that a better optical performance can be achieved at a large injection current. All the above advantages are due to the significant enhancement of the carriers and the much smaller polarization field in the active region.

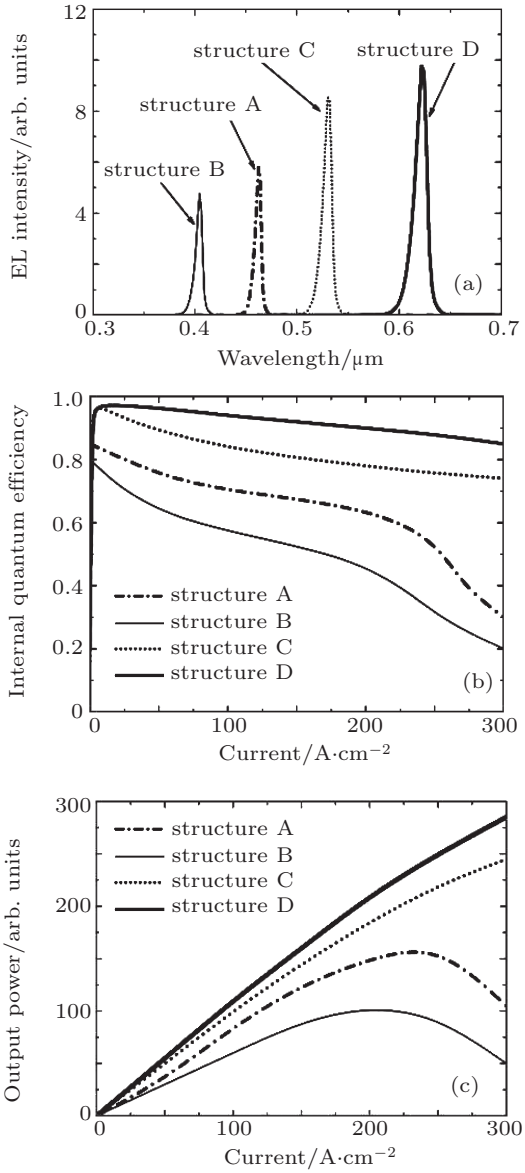


Fig. 4. (a) The EL spectra of the LEDs at an injection current of 150 mA (the peaks are shifted for better observation), (b) IQE versus injection current and (c) output power versus injection current for the LEDs.

4. Conclusion

We compared LEDs with four different EBL structures by simulating the emission spectra, the electron and hole concentrations, the energy band diagrams, the electrostatic fields, and the internal quantum efficiencies. The results indicate that hole injection efficiency can be greatly improved when the AlGaN EBL with gradually increasing Al content is adopted. This can also effectively suppress electrons spilling over from the active region because of the higher effective potential height for the electrons. It is proved that the LED with this specifically designed EBL structure has significantly better optical performance, such as a lower efficiency droop, a bigger EL luminous intensity, and larger output power even under large injection current conditions.

References

[1] Bergh A, Craford G, Duggal A and Haitz R 2001 *Phys. Today* **5544** 42
[2] Mathew C, Schmid T, Kim K C, Hitoshi S, Natalie F, Hisashi M, Shuji N, Steven P D and James S S 2007 *Jpn. J. Appl. Phys.* **46** L126
[3] Chen G, Craven M, Kim A, Munkholm A, Watanabe S, Camras M, Götz W and Steranka F 2008 *Phys. Status Solidi* A **205** 1086
[4] Li Y L, Huang Y R and Lai Y H 2007 *Appl. Phys. Lett.* **91** 181113
[5] Kim M H, Schubert M F, Dai Q, Kim J K, Schubert E F, Piprek J and Park Y 2007 *Appl. Phys. Lett.* **91** 183507
[6] Schubert M F, Xu J, Kim J K, Schubert E F, Kim M H, Yoon S, Lee S M, Sone C, Sakong T and Park Y 2008 *Appl. Phys. Lett.* **93** 041102
[7] David A, Grundmann M J, Kaeding J F, Gardner N F, Mihopoulos T G, Krames M R, Mihopoulos T G and Krames M R 2008 *Appl. Phys. Lett.* **92** 053502
[8] Chen Y X, Shen G D, Han J R, Li J J and Guo W L 2010 *Acta Phys. Sin.* **59** 545 (in Chinese)
[9] Xing Y H, Han J, Deng J, Li J J, Xu C and Shen G D 2010 *Acta Phys. Sin.* **59** 1233 (in Chinese)
[10] Zhang Y Y and Fan G H 2011 *Chin. Phys.* B **20** 048502
[11] Efremov A A, Bochkareva N I, Gorbunov R I, Larinovich D A, Rebane Y T, Tarkhin D V and Shreter Y G 2006 *Semiconductors* **40** 605
[12] Shen Y C, Müller G O, Watanabe S, Gardner N F, Munkholm A and Krames M R 2007 *Appl. Phys. Lett.* **91** 141101
[13] Gardner N F, Müller G O, Shen Y C, Chen G, Watanabe S, Götz W and Krames M R 2007 *Appl. Phys. Lett.* **91** 243506
[14] Kim A Y, Götz W, Steigerwald D A, Wierer J J, Gardner N F, Sun J, Stockman S A, Martin P S, Krames M R, Kern R S and Steranka F M 2001 *Phys. Status Solidi* A **188** 15
[15] Chichibu S F, Azuhata T, Sugiyama M, Kitamura T, Ishida Y, Okumurac H, Nakanishi H, Sota T and Mukai T 2001 *J. Vac. Sci. Technol.* B **19** 2177
[16] Xie J, Ni X, Fan Q, Shimada R, Ozgur U and Morkoc H 2008 *Appl. Phys. Lett.* **93** 121107
[17] Pope I A, Smowton P M, Blood P, Thomson J D, Kappers M J and Humphreys C J 2003 *Appl. Phys. Lett.* **82** 2755

[18] Wang B, Li Z, Yao R, Liang M, Yan F W and Wang G H 2011 *Acta Phys. Sin.* **60** 016108 (in Chinese)

[19] Chen H, Ding G J, Guo L W, Jia H Q, Liu J, Liu X Y, Lv L, Tan C L, Xing Z G, Zhou J M and Zhou Z T 2007 *Acta Phys. Sin.* **56** 6013 (in Chinese)

[20] Zhao D G, Zhou M and Zuo S H 2007 *Acta Phys. Sin.* **56** 5513 (in Chinese)

[21] Duan H T, Hao Y, Xu Z H, Zhang J C, Zhang Z F and Zhu Q W 2009 *Chin. Phys.* B **18** 5457

[22] Chen J F and Hao Y 2009 *Chin. Phys.* B **18** 5451

[23] Liu N X, Wang H B, Liu J P, Niu N H, Han J and Shen G D 2006 *Acta Phys. Sin.* **55** 1424 (in Chinese)

[24] Cao Z Y, Cu W P, Hao Y, Li P X and Zhang J C 2009 *Chin. Phys.* B **18** 4970

[25] Chen G F, Jiang D S, Liu Z S, Wang H, Wang Y T, Wu Y X, Yang H, Zhang S M, Zhao D C and Zhu J 2009 *Chin. Phys.* B **18** 4413

[26] Feng Q, Hao Y and Wang F X 2004 *Acta Phys. Sin.* **53** 3587 (in Chinese)

[27] Lee J, Li X, Ni X, Özgür U, Morkoç H, Paskova T, Mulholland G and Evans K R 2009 *Appl. Phys. Lett.* **95** 201113

[28] APSYS by Crosslight Software Inc. (http://www.crosslight.com)

[29] Kuo Y K, Chang J Y, Tsai M C and Yen S H 2009 *Appl. Phys. Lett.* **95** 011116

[30] Piprek J and Nakamura S 2002 *IEEE Proc. J. Optoelectron.* **149** 145

[31] Vurgaftman I and Meyer J R 2003 *J. Appl. Phys.* **94** 3675

[32] Kuo Y K, Wang T H, Chang J Y and Tsai M C 2011 *Appl. Phys. Lett.* **99** 091107